Supporting Information

Manganese Doped Carbon Dots as a Promising Nanoprobe for Luminescent and Magnetic Resonance Imaging

Evgeniia A. Stepanidenko [1,*], Anna A. Vedernikova [1], Zilya F. Badrieva [2], Ekaterina A. Brui [2], Saikho O. Ondar [1,3], Mikhail D. Miruschenko [1], Olga V. Volina [4], Aleksandra V. Koroleva [4], Evgeniy V. Zhizhin [4], Elena V. Ushakova [1]

[1] International Research and Education Centre for Physics of Nanostructures, ITMO University, 197101 Saint Petersburg, Russia
[2] Engineering and Physical Faculty, ITMO University, 197101 Saint Petersburg, Russia
[3] Saint-Petersburg State Institute of Technology, 190013 Saint-Petersburg, Russia
[4] Research Park, Saint Petersburg State University, 199034 Saint Petersburg, Russia

*Correspondence: eastepanidenko@itmo.ru

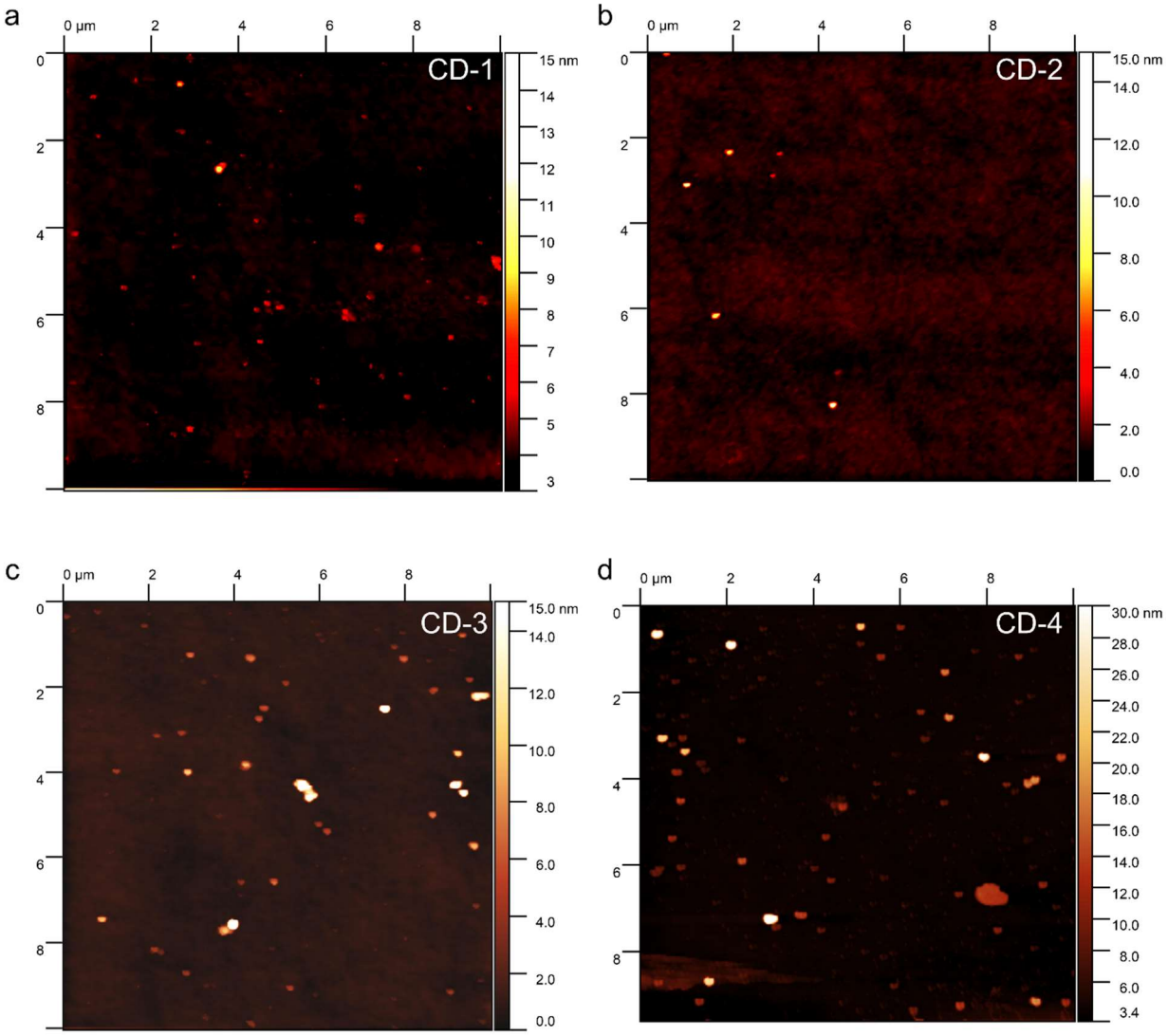

Figure S1. Additional AFM images of CD samples.

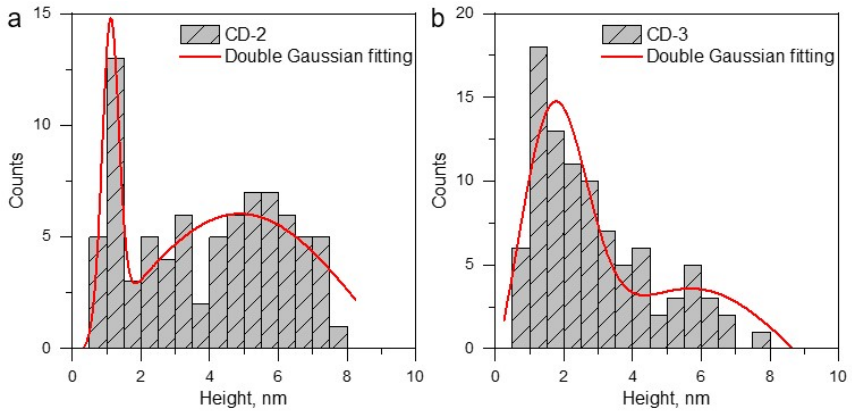

Figure S2. The height distributions for CD-2 (a) and CD-3 (b) fitted by Double Gaussian function.

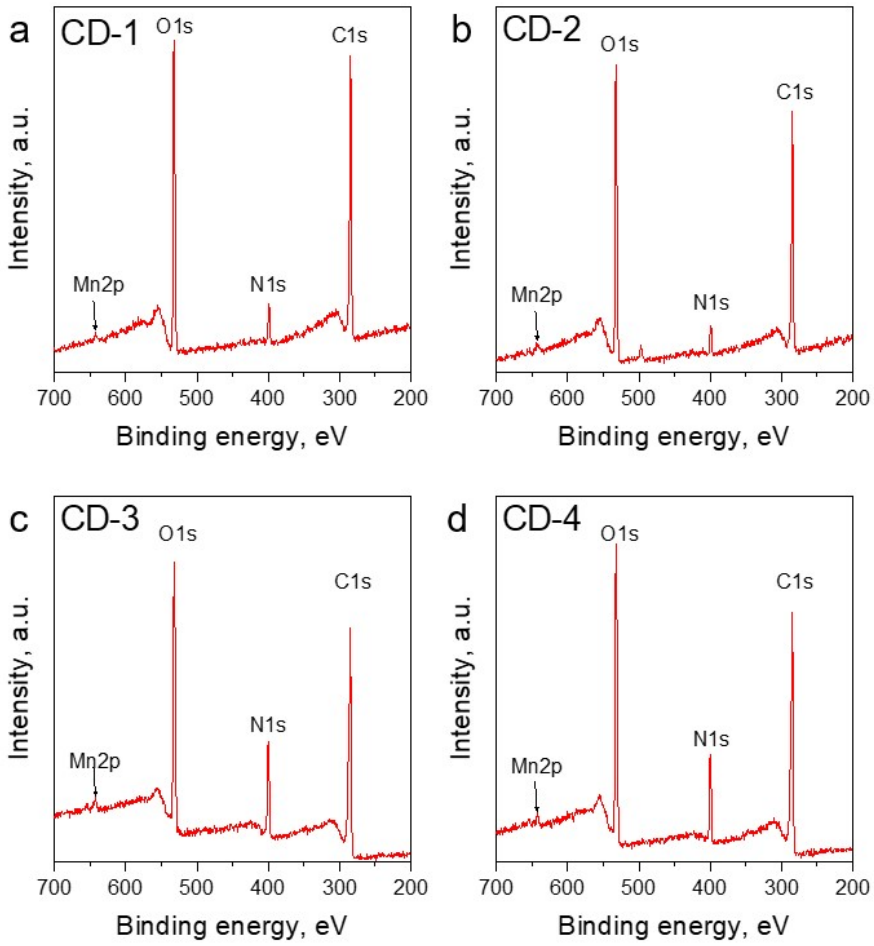

Figure S3. Full X-ray photoelectron spectroscopy (XPS) survey spectra of CD-1 (a), CD-2 (b), CD-3 (c), and CD-4 (d).

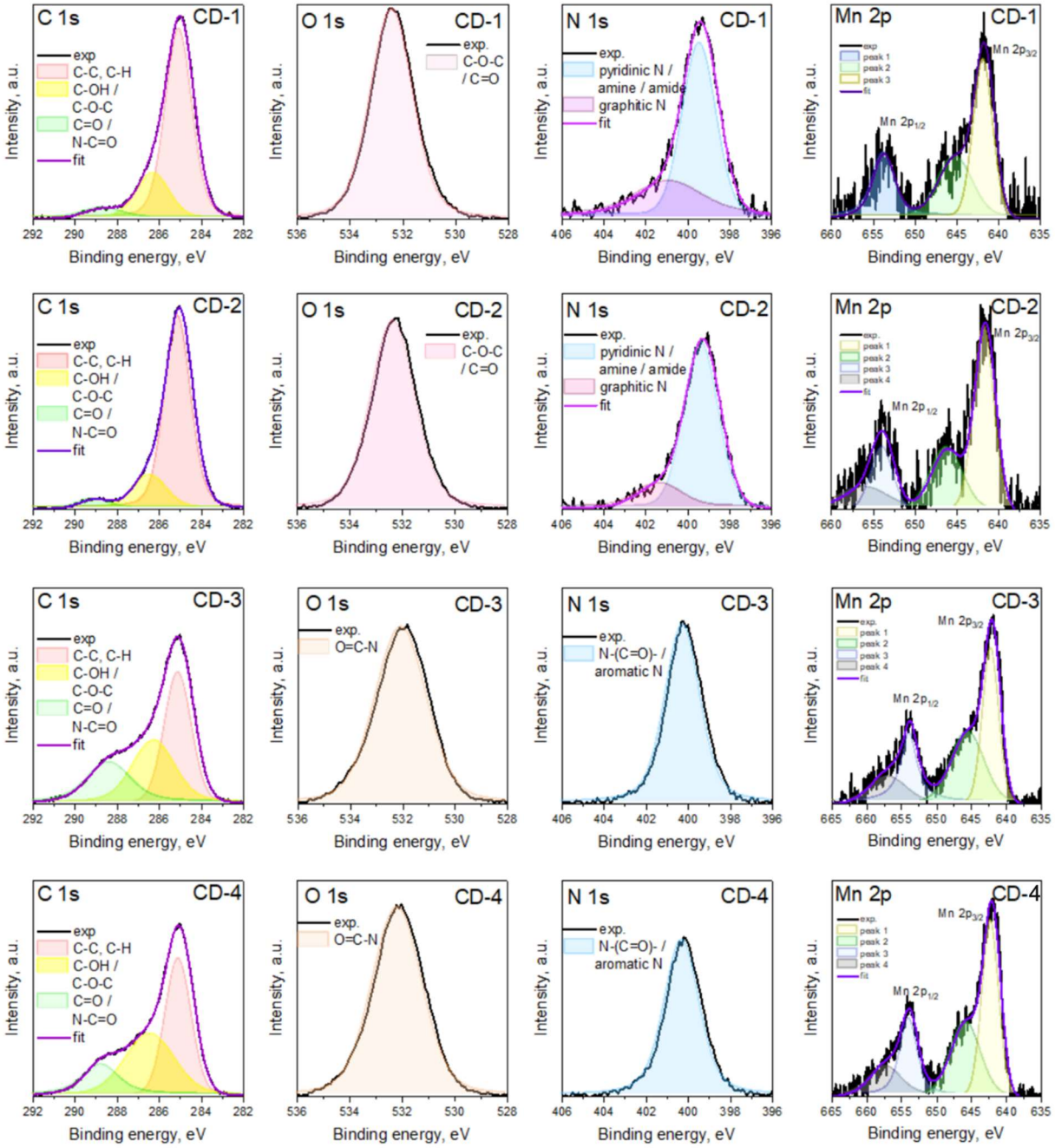

Figure S4. High-resolution XPS spectra of Mn-doped CDs: C 1s (1st left row), O 1s (2nd row), N 1s (3rd row) and Mn 2p (4th right row), with deconvolution of bands to specific peaks attributed to different chemical groups shown by different colors and explained in the legends. For Mn 2p, peak 1 at 641.8-642.0 eV and peak 3 at 653.7-653.9 eV are attributed to Mn(IV) compounds, peak 2 at 645.1-646.0 eV and peak 4 at 656.1-657.2 eV are attributed to Mn(VII) compounds.

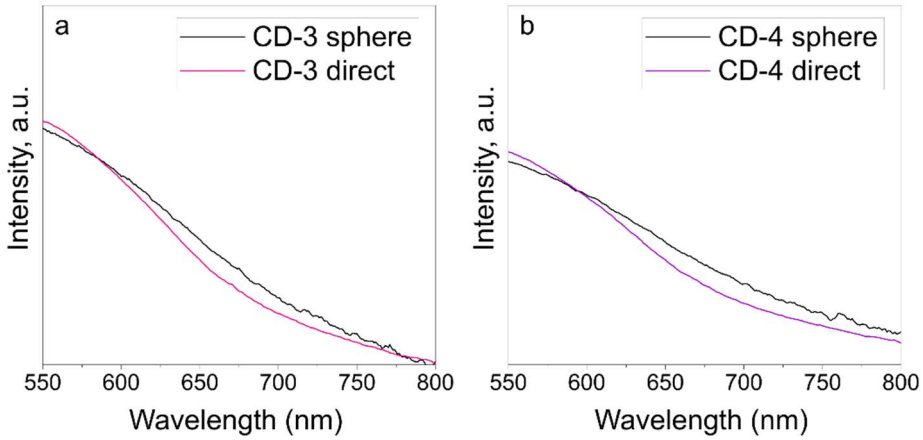

Figure S5. Optical spectra measured in a direct mode (pink and purple lines) and using an integrating sphere (black lines). The first spectra are attributed to absorption and the latter ones are sum of absorption and reflection. It is seen that the signals in the 600-800 nm spectral region are almost the same, thus, the optical density in the 600-700 nm spectral region originates from absorption by CDs.

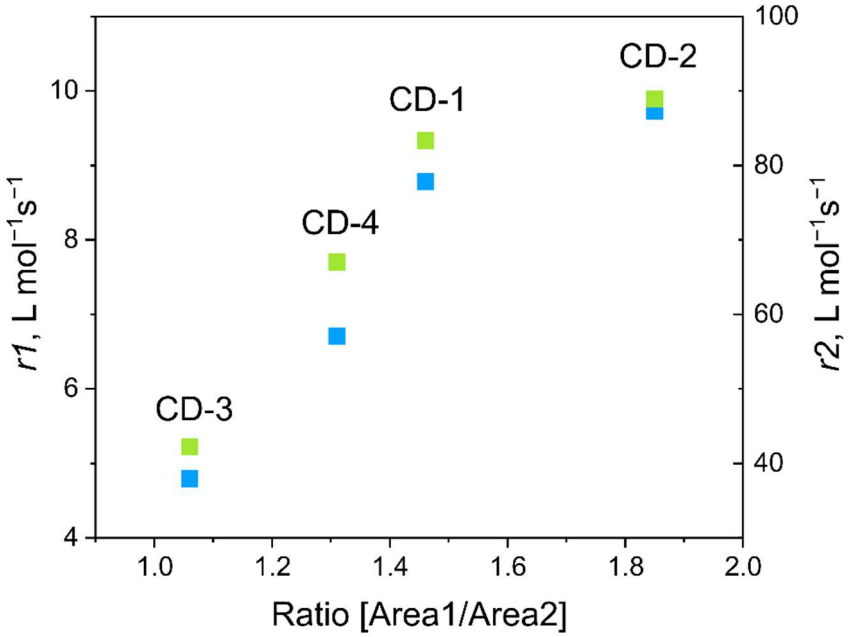

Figure S6. Dependence of *r1* (blue squares) and *r2* (light green squares) relaxivities on the ratio of the peak 1 and peak 2 in Mn $2p_{3/2}$ band areas taken from Table S3.

Table S1. Synthesis conditions and composition of CDs

Sample	Precursor, amount (g)		Solvent	Synthesis parameters and purification	Atomic (%)			
					C	O	N	Mn
CD-1	o-phenylenediamine	0.3	Ethanol, 10 mL	180°C, 12h Dialysis 1 day 3.5 kDa	64.49	28.48	6.66	0.37
	$Mn(Ac)_2$	0.2						
CD-2	o-phenylenediamine	0.3			67.88	27.27	4.44	0.41
	$MnCl_2$	0.1						
CD-3	citric acid	0.5	Formamide, 5 mL	180°C, 12h Precipitation in EtOH Dialysis 1 day 3.5 kDa	61.80	24.50	13.00	0.70
	$Mn(Ac)_2$	0.127						
CD-4	citric acid	0.5			61.40	26.10	11.70	0.80
	$MnCl_2$	0.065						

Table S2. Height distribution of CDs from statistical analysis of AFM images

Sample	Total number of analyzed particles	Mean value, nm	Median value, nm
CD-1	101	1.9±1.3	1.5
CD-2	100	5.7±3.5	5.7
CD-3	100	3.5±2.7	2.6
CD-4	100	2.8±2.3	1.8

Table S3. Optical properties of CDs

Sample	Absorption peak, nm	PLE peak, nm	PL peak, nm
CD-1	258 418	255 324 418	570 368 567
CD-2	258 418	255 320 420	570 368 567
CD-3	527	270 380-430 550	430-500 460-500 620
CD-4	537	270 380-420 550	430-500 460-500 620

Table S4. Deconvolution parameters for Mn $2p_{3/2}$ band

	OPD-based CDs		**CA-based CDs**	
	CD-1	**CD-2**	**CD-3**	**CD-4**
	$Mn(Ac)_2$	**$MnCl_2$**	**$Mn(Ac)_2$**	**$MnCl_2$**
1st peak position, eV	641.7	641.6	642.0	642.0
1st peak area (Area 1)	416.8	506.2	874.3	1025.8
2nd peak position, eV	645.1	646.1	645.4	645.6
2nd peak area (Area 2)	284.8	273.2	824.6	784.5
Area1/Area2	1.46	1.85	1.06	1.31

Table S5. Characteristics of Mn-based contrast agents

Contrast agent	*r1*, L mmol^{-1} s^{-1}	*r2*, L mmol^{-1} s^{-1}	Magnetic field strengths, T	Media	Ref.
Teslascan ™	3.6	7.1	1.5 T	plasma at 37°C	[1]
Mn-doped CDs	6.23		7 T		[2]
Mn-CDs-NHF[1]	17.75 mg^{-1}mL s^{-1}	88.60 mg^{-1}mL s^{-1}	1 Tesla	1% agarose gel	[3]
PEG-MnO NPs [2,3]	12.942	60.26	3.0 T	1% agarose gel	[4]
Mn-DMSS[4]	10.1	169.7	3.0 T	pure water	[5]
Mn complex [5]	4.88 5.2		9.4 1.5	50 mM HEPES buffer at pH 7.0,	[6]
PDA@N-CDs(Mn)[6]	14.15	39.2	3.0 T	PBS buffer	[7]
Mn-doped CDs	7.28		1,2		[8]
Mn-NGQDs [7]	15.86	177.51	1.5	aqueous suspension	[9]
Mn@CQDs [8]	7.43	140.7	7.0	PBS buffer	[10]
Mn-doped CDs	12.69		0.5		[11]
Mn-doped CDs	8.79 9.74 4.80 6.71	83.39 88.95 42.24 67.06	1.5	9% saline solution	This work

[1] NHF – N-Hydroxyphthalimide-derived, [2] PEG – Polyethylene glycol, [3] NPs – nanoparticles, [4] DMSS – Dual-mesoporous silica spheres, [5] 2,6-diacetylpyridine bisacetylhydrazone complex, [6] N-doped carbon dots (N-CDs) embedded onto Mn^{2+} complex-modified polydopamine (PDA), [7] NGQDs – nitrogen co-doped graphene quantum dots.

References

1. Pintaske, J.; Martirosian, P.; Graf, H.; Erb, G.; Lodemann, K.P.; Claussen, C.D.; Schick, F. Relaxivity of Gadopentetate Dimeglumine (Magnevist), Gadobutrol (Gadovist), and Gadobenate Dimeglumine (MultiHance) in Human Blood Plasma at 0.2, 1.5, and 3 Tesla. *Invest Radiol* **2006**, *41*, doi:10.1097/01.rli.0000197668.44926.f7.

2. Ji, Z.; Ai, P.; Shao, C.; Wang, T.; Yan, C.; Ye, L.; Gu, W. Manganese-Doped Carbon Dots for Magnetic Resonance/Optical Dual-Modal Imaging of Tiny Brain Glioma. *ACS Biomater Sci Eng* **2018**, *4*, 2089–2094, doi:10.1021/acsbiomaterials.7b01008.

3. Tiron, A.; Stan, C.S.; Luta, G.; Uritu, C.M.; Vacarean-Trandafir, I.-C.; Stanciu, G.D.; Coroaba, A.; Tiron, C.E. Manganese-Doped N-Hydroxyphthalimide-Derived Carbon Dots—Theranostics Applications in Experimental Breast Cancer Models. *Pharmaceutics* **2021**, *13*, 1982, doi:10.3390/pharmaceutics13111982.

4. Li, J.; Wu, C.; Hou, P.; Zhang, M.; Xu, K. One-Pot Preparation of Hydrophilic Manganese Oxide Nanoparticles as T1 Nano-Contrast Agent for Molecular Magnetic Resonance Imaging of Renal Carcinoma in Vitro and in Vivo. *Biosens Bioelectron* **2018**, *102*, doi:10.1016/j.bios.2017.10.047.

5. Niu, D.; Luo, X.; Li, Y.; Liu, X.; Wang, X.; Shi, J. Manganese-Loaded Dual-Mesoporous Silica Spheres for Efficient T1- and T2-Weighted Dual Mode Magnetic Resonance Imaging. *ACS Appl Mater Interfaces* **2013**, *5*, doi:10.1021/am401856w.

6. Anbu, S.; Hoffmann, S.H.L.; Carniato, F.; Kenning, L.; Price, T.W.; Prior, T.J.; Botta, M.; Martins, A.F.; Stasiuk, G.J. A Single-Pot Template Reaction Towards a Manganese-Based T1 Contrast Agent. *Angewandte Chemie - International Edition* **2021**, *60*, doi:10.1002/anie.202100885.

7. Zhang, M.; Zheng, T.; Sheng, B.; Wu, F.; Zhang, Q.; Wang, W.; Shen, J.; Zhou, N.; Sun, Y. Mn2+ Complex-Modified Polydopamine- and Dual Emissive Carbon Dots Based Nanoparticles for in Vitro and in Vivo Trimodality Fluorescent, Photothermal, and Magnetic Resonance Imaging. *Chemical Engineering Journal* **2019**, *373*, doi:10.1016/j.cej.2019.05.107.

8. Wang, Y.; Wang, T.; Chen, X.; Xu, Y.; Li, H. Mn(II)-Coordinated Fluorescent Carbon Dots: Preparation and Discrimination of Organic Solvents. *Opt Mater (Amst)* **2018**, *78*, doi:10.1016/j.optmat.2018.02.026.

9. Lee, B.H.; Hasan, M.T.; Lichthardt, D.; Gonzalez-Rodriguez, R.; Naumov, A. V. Manganese-Nitrogen and Gadolinium-Nitrogen Co-Doped Graphene Quantum Dots as Bimodal Magnetic Resonance and Fluorescence Imaging Nanoprobes. *Nanotechnology* **2021**, *32*, doi:10.1088/1361-6528/abc642.

10. Yao, Y.Y.; Gedda, G.; Girma, W.M.; Yen, C.L.; Ling, Y.C.; Chang, J.Y. Magnetofluorescent Carbon Dots Derived from Crab Shell for Targeted Dual-Modality Bioimaging and Drug Delivery. *ACS Appl Mater Interfaces* **2017**, *9*, doi:10.1021/acsami.7b01599.

11. Sun, S.; Zhao, L.; Wu, D.; Zhang, H.; Lian, H.; Zhao, X.; Wu, A.; Zeng, L. Manganese-Doped Carbon Dots with Redshifted Orange Emission for Enhanced Fluorescence and Magnetic Resonance Imaging. *ACS Appl Bio Mater* **2021**, *4*, 1969–1975, doi:10.1021/acsabm.0c01597.